Supporting Information

Hot-electron Transfer Promotes Ion Production in Plasmonic Metal Nanostructure Assisted Laser Desorption Ionization Mass Spectrometry

Yafeng Li[a,b], Xiaohua Cao[a], Lingpeng Zhan[b,c], Jinjuan Xue[b,c], Jiyun Wang[b], Huihui Liu[b], Caiqiao Xiong[b], and Zongxiu Nie*[b.c,d]

[a] College of Chemical and Environmental Engineering, Jiujiang University, Jiujiang, Jiangxi Province, 332005

[b] Beijing National Laboratory for Molecular Sciences, Key Laboratory for Analytical Chemistry for Living Biosystems, Institute of Chemistry, Chinese Academy of Sciences, Beijing, 100190, China.

[c] University of Chinese Academy of Sciences, Beijing, 100049, China.

[d] National Centre for Mass Spectrometry in Beijing, Beijing, 100190, China.

Abstract. The supporting information includes 1 scheme and 8 figures, experimental details and some additional discussions. Scheme S1 is the illustration of LSPR generated around isolated AgNPs and aggregated AgNPs upon the irradiation of the same laser. Figure S1 UV-Vis absorption spectrum of AgNPs which was used as comparison materials in our work. Figure S1 is the UV-Vis absorption spectrum of conventional AgNPs which was used as comparison materials in our work. Figure S2 is the mass spectra of tetraphenylborate anions detected with AgNI-on-ND and AgNP (silver concentrations are the same) respectively on nonconducting glass substrate. Figure S3 is the detailed generation pathways of ion 1-5 in Figure 4. Figure S4 is the enlarged view of the mass spectrum of Asp detected by using AgNI-on-ND as LDI-assisting material. Figure S5 is the TEM image of AuNP and its UV-Vis spectrum. Figure S6 is the LDI MS result (negative mode) of Asp using AuNP as LDI-assisting materials. Figure S7 is the LIFT MSMS analysis of Juglone dimer $[M-2H]^{\bullet-}$ m/z 346. Figure S8 is the Raman spectra of 0.1 mM Rhodamine 6G on AgNP and AgNI-on-ND respectively.

Supplementary Figures:

Scheme S1: Illustration of LSPR generated around isolated AgNPs and aggregated AgNPs upon the irradiation of the same laser.

Figure S1: UV-Vis absorption spectrum of AgNPs which was used as comparison materials in our work.

Figure S2: mass spectra of tetraphenylborate anions detected with AgNI-on-ND and AgNP (silver concentrations are the same) respectively on nonconductive glass substrate.

Figure S3. Detailed generation pathways of ion 1-5 in Figure 4.

Figure S4. Enlarged view of the mass spectrum of Asp detected by using AgNI-on-ND as LDI-assisting material.

Figure S5. TEM image of AuNP (top) and its UV-Vis spectrum (bottom).

Figure S6. LDI MS result (negative mode) of Asp using AuNP as assisting materials.

Figure S7. LIFT MSMS analysis of Juglone dimer $[M-2H]^{\bullet -}$ m/z 346.

Figure S8. Raman spectra of 0.1 mM Rhodamine 6G on AgNP and AgNI-on-ND respectively.

Experimental Details

Materials. Deionized water was provided by a Mili-Q Integral water purification system. Pyrogallol (PG) and bicine were purchased from J&K. Aspartic acid, sodium tetraphenylborate, juglone and acetic acid were provided by Sigma-Aldrich (St Louis, USA). $AgNO_3$ was purchased from Sinopharm Chemical Reagent Co., Ltd.

Aspartic acid (1 mM and 10 mM), sodium tetraphenylborate (1 mM) were dissolved in MeOH:H_2O 1:1 (v:v); Juglone was dissolved in Acetone, and the concentration was 2 ppm.

Fabrication of AgNI-on-ND, AgNPs and AuNPs. AgNI-on-ND was fabricated through a bio-inspired surface coating method. It is a kind of surface modification approach which utilizes some bio-inspired "sticky" molecules to transform the original surface to a multifunctional surface. This method is simple, only two dip-coating steps are needed to synthesize AgNI-on-ND. The bio-inspired "sticky" molecule we are using in this work is Pyrogallol, which is rich in tea, chocolate, and wine.

Nanodiamond with an average size of 100 nm was first suspended in deionized water with a concentration of 1 mg/ml. For deposition of adherent PG layer, 0.5 mL of the material suspension was first centrifuged and supernatant water was removed. Then 500 μL 0.1 mg/mL PG, pH 7.8 (100 mM bicine) was added, and the suspension was sonicated for 20 min. The addition of 500 μL 1 mM $AgNO_3$ was then followed, and the suspension was sonicated for another 10 min. Ten μL of 12 mM acetic acid was added to stop the reaction. The final suspension was then centrifugated and washed with 1 mL water, and finally suspended in 1 mL deionized water for use. So the final concentration of AgNI-on-ND was 0.5 mg/mL (based on ND concentrations), and the concentration of silver was 0.5 mM (concentration of silver atom).

For comparison experiments, PG reduced AgNPs were synthesized by the same procedure as preparing AgNI-on-ND without adding ND materials. UV-Vis of thus prepared AgNPs is shown in Figure S2.

The brief AuNP synthesis process was: 50 mL of 1 mM $HAuCl_4$ was boiling with vigorous stirring, then 5 mL of 38.8 mM sodium citrate was rapidly added to the above solution and kept boiling for another 10 min to get a wine-red solution, then stopped heating and cooled to room temperature. Before use, the AuNP solution was diluted to 0.5 mM (concentration of gold atom), centrifuged and washed by DI water twice, and then suspended in DI H_2O.

Mass spectrometry analysis. LDI analysis was performed on a Bruker Ultraflextreme LDI-TOF/TOF mass spectrometer (Bruker Daltonics, Billerica, MA) equipped with a smartbeam Nd: YAG 355 nm laser with reflection in negative ion mode. The maximum laser energy (outlet) was 100 μJ, and can be adjusted between 0% and 100%. During all the testing, 15%-30% energy, 1000 Hz, 200 shots were used unless otherwise stated.

Ultraviolet-visible (UV-Vis) spectrometer and Transmission electron microscope (TEM)： The UV-Vis spectrometer used here was TU-1900 Spectrometer (Beijing, China). The TEM used for AuNP characterizing was Hitachi HT7700, and JEM-2011 for other material characterization.

Raman analysis. Raman analysis was performed on a RENISHAW Via-Reflex Raman system with a 785 nm excitation wavelength operating at 1 mW. Rhodamine 6G of 0.1 mM were mixed with 0.25 mM AgNI-on-ND (concentration of silver atom) and 0.25 mM AgNP (concentration of silver atom) respectively before dropcasting onto Raman substrate.

Discussion:

LSPR-induced photo-thermal effect:

Nanomaterial-assisted LDI desorption process has been widely acknowledged as a laser-induced thermal desorption process [4]. Due to LSPR effect, silver nanostructures have higher UV laser absorption efficiency than many other non-plasmonic nanostructures. By comparing the desorption efficiency of a preformed ion, tetraphenylborate, on different nanomaterials, as is shown in Figure 2a, we can see that silver nanostructures have much

higher desorption efficiencies than ND-related materials. This can be regarded as a proof of the LSPR-induced photo-thermal effect.

Upon laser irradiation, the local temperature around AgNI can be very high. We can use some equations to estimate the temperature. Assume that the energy of a specified laser fluence (Φ, in J cm^{-2}) absorbed by the AgNI (Q_{abs}) is converted into the density of internal absorbed energy (E, in J cm^{-3}), and the internal absorbed energy is then totally converted into heat, thus the maximum temperature that the AgNI can achieve at the specified laser fluence can be calculated by the following two equations:

$$E = \frac{3Q_{abs}}{4\ R}\Phi$$

$$E = C\rho T$$

Where C is the heat capacity of silver (0.235 J $g^{-1}K^{-1}$), ρ is the density of silver (10.5 g cm^{-3}, 298K), and T is the laser-induced heating temperature of AgNI. Q_{abs} can be calculated based on the Rayleigh approximation [5],

$$Q_{abs} = q\frac{12\varepsilon^{''}}{(\varepsilon^{'}+2)^2+\varepsilon^{''2}}$$

Here, ε' stands for the real part of the dielectric permittivity (ε) of silver (-2.04), and ε'' represents the imaginary part (0.28). And the calculation result is 0.18525.

For the laser fluence we used in our experiments (around 40 mJ cm^{-2}), the calculated T is 14269 K.

In fact, the laser energy absorbed by AgNI has several other ways of dissipation, such as radiation and the generation of energetic charge carriers, etc. Local heating is only part of it. So the local temperature should be much less than 14269 K, but still high enough to desorb the analyte molecules.

Molecules adsorbed on LDI-assisting materials are desorbed upon laser pulse irradiation mainly through laser-induced heat effect. For ND-related materials, the laser-induced heat effect is small, resulting in a low analyte desorption efficiency (as is shown in Figure 2a). For silver nanostructure, as the laser pulse excites the LSPR effect, the energy of which would partially decay through thermal dissipation, the laser-induced heat effect is much stronger compared with that of the ND-related materials, resulting in a very high analyte desorption efficiency (as is shown in Figure 2a).

Possible applications of AgNIs in mass spectrometric practice.

For regular sample analysis, as AgNI-on-ND outperforms both NDs and AgNPs, it would be an excellent alternative for LDI MS analysis.

As AgNI generates hot electrons effectively upon laser irradiation, and the hot electrons can not only catalyze chemical reactions but also ionize the reactants and the products, it would be very suitable to be applied to do on-line monitoring of hot electron catalyzed reactions.

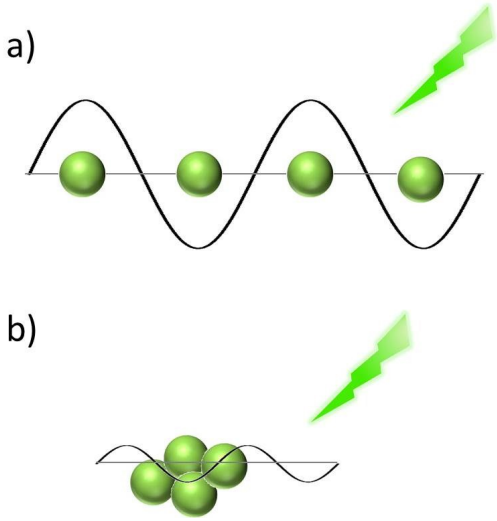

Scheme S1. Illustration of LSPR of a) isolated AgNPs and b) aggregated AgNPs generated upon the irradiation of the same laser (say 355 nm). When AgNPs are isolated, the LSPR can be effectively excited; when they cluster together, the LSPR becomes very weak.

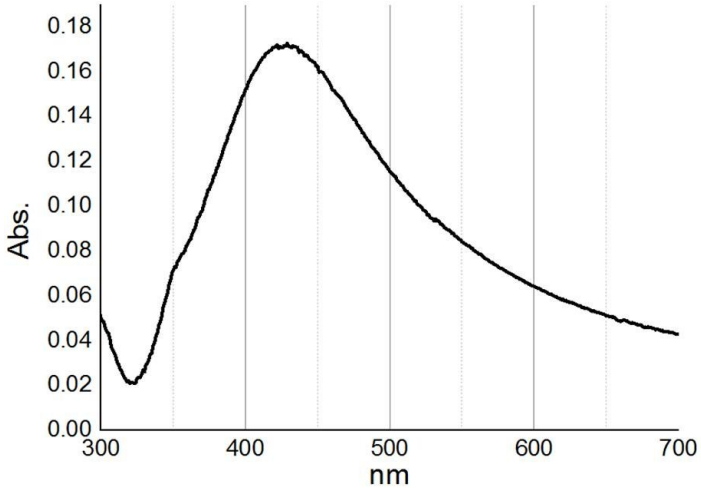

Figure S1. UV-Vis absorption spectrum of AgNPs.

The absorption band profile of AgNI in Fig 1b and AgNP in Fig S1 look similar because the UV-Vis of both materials were all detected in suspensions. No aggregations were formed in solution phase for both cases. But when AgNP suspension was dropcast onto LDI substrate, AgNPs would aggregate during solvent evaporation process. For AgNI-on-ND, the ND acted as AgNI holder which prevented the aggregation of AgNIs during drying process on the plate.

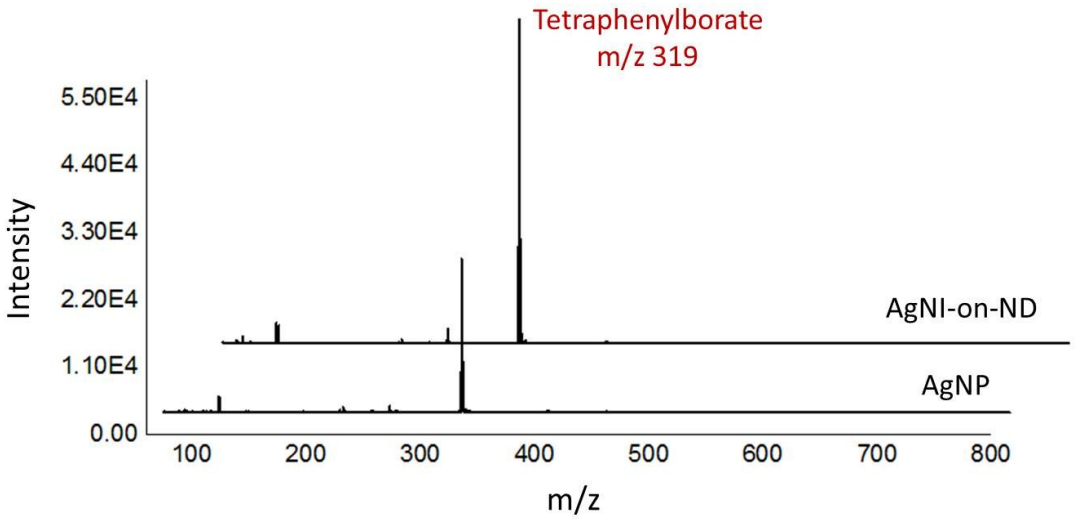

Figure S2. Mass spectra of tetraphenylborate anions detected with AgNI-on-ND and AgNP respectively on nonconductive glass substrate. The silver concentrations were the same in the two nanomaterials.

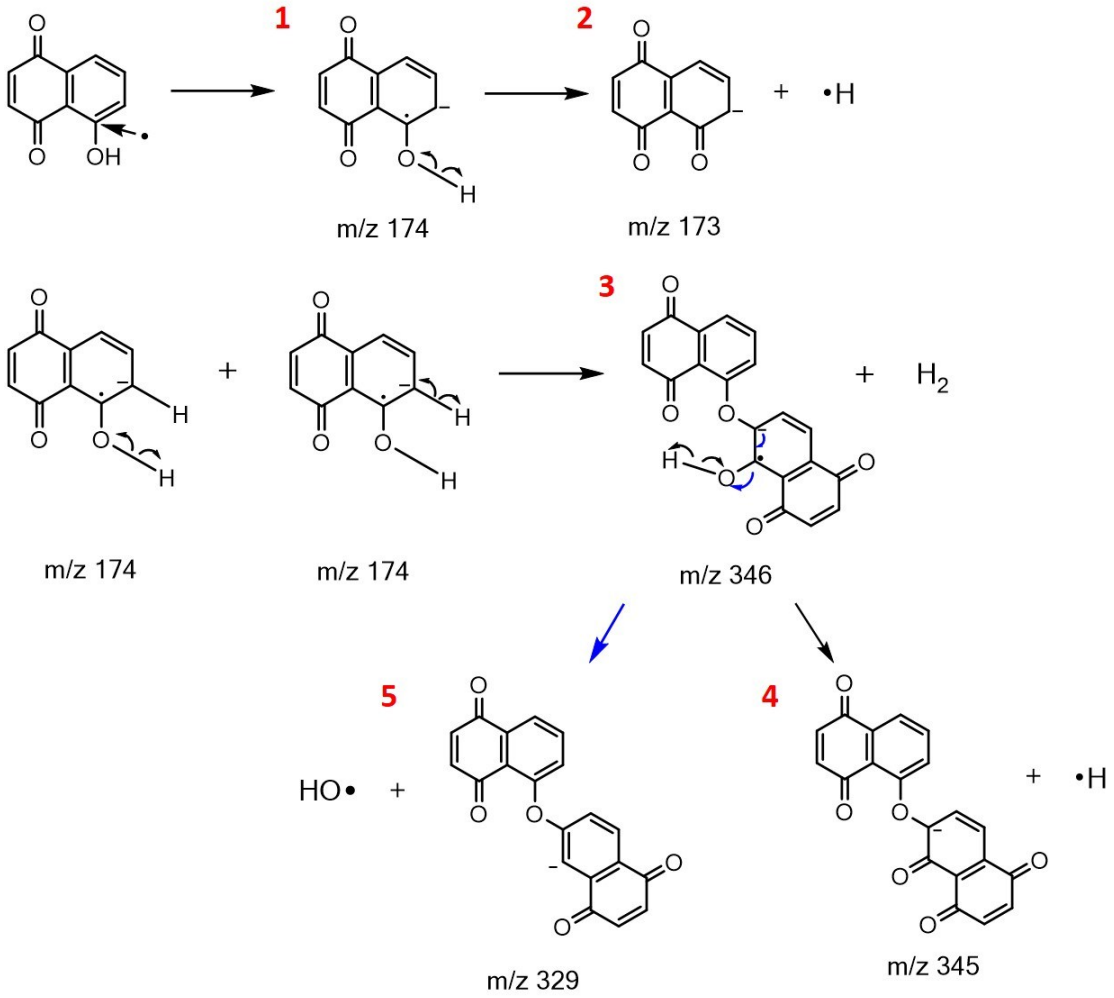

Figure S3. Detailed generation pathways of juglone-related ion 1-5 in Figure 4.

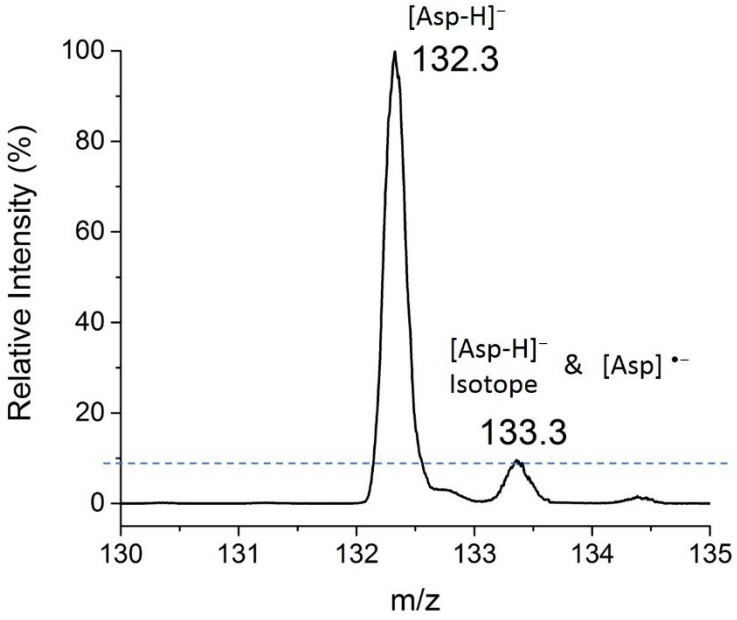

Figure S4. Enlarged view of the mass spectrum of Asp detected by using AgNI-on-ND as LDI-assisting material.

Although the electron affinity of Asp is much weaker than Juglone, the radical ion, $[Asp]^{\bullet-}$ (m/z 133) was still generated and observed. As is shown in Figure S4, the relative intensity of $[Asp\text{-}H]^-$ (m/z 132) is 100%, while the relative intensity of m/z 133 is about 8.7%, which is much higher than the theoretical isotope abundance of $[Asp\text{-}H]^-$ (4.9%), indicating the existence of the radical ion, $[Asp]^{\bullet-}$(m/z 133).

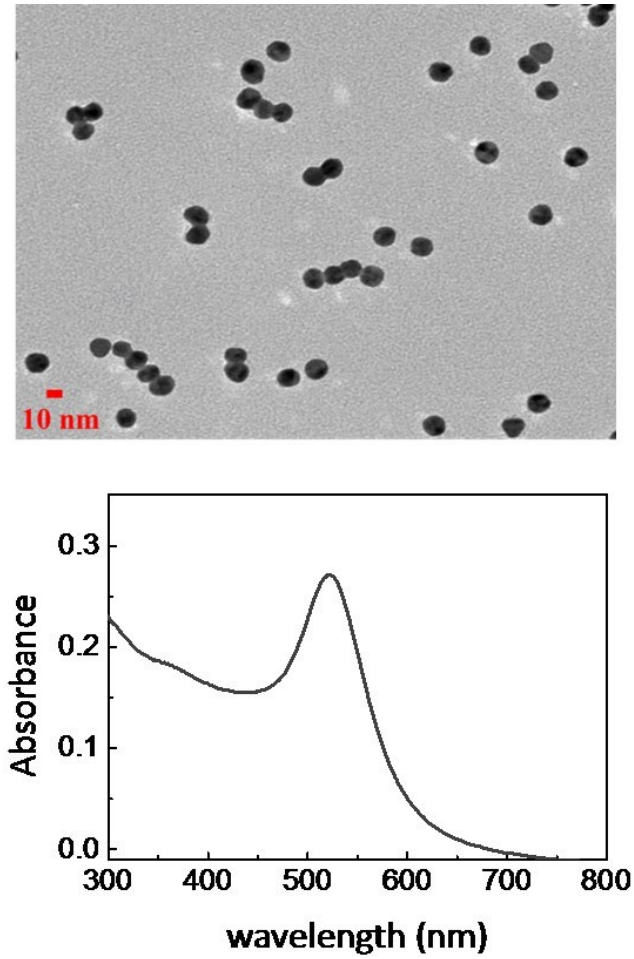

Figure S5. TEM image of AuNP (top) and its UV-Vis spectrum (bottom).

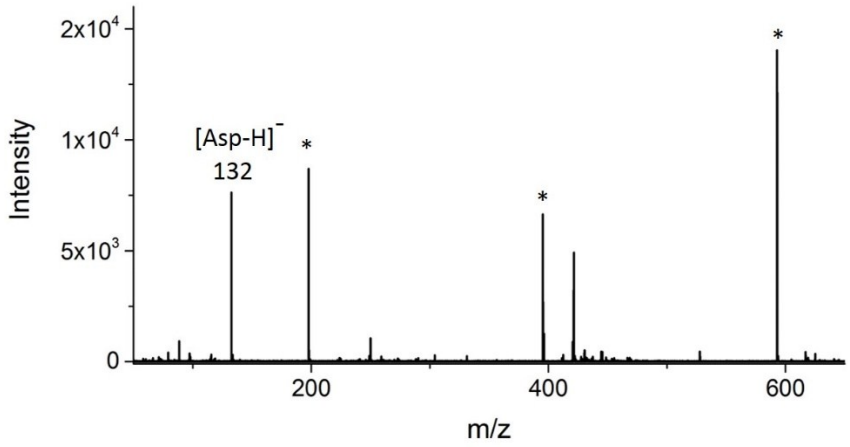

Figure S6. LDI MS result (negative mode) of Asp using AuNP as LDI-assisting materials. Nonconducting glass was used as substrate. Asterisks (*) indicate Au_n^- signals.

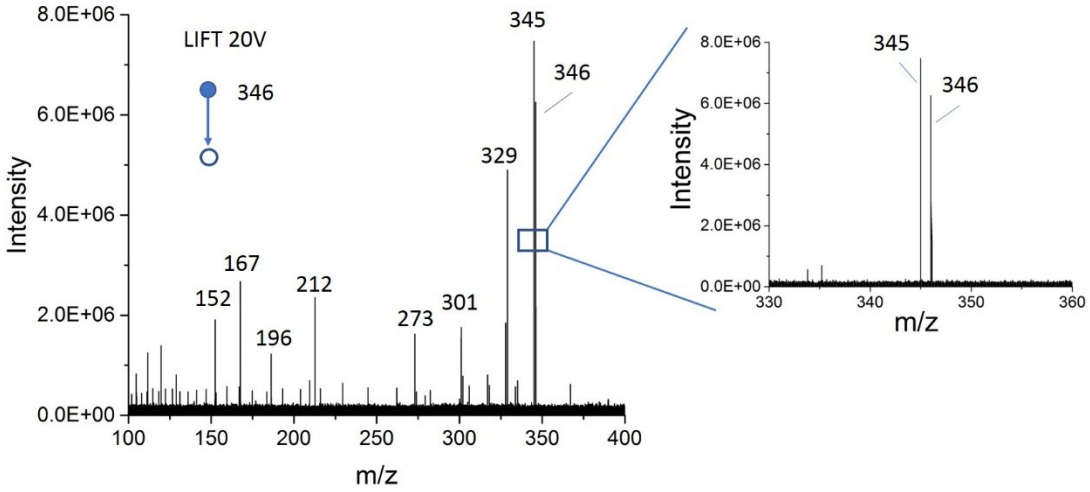

Figure S7. LIFT MSMS analysis of Juglone dimer $[M-2H]^{\bullet -}$ m/z 346.

Laser-induced polymerization can occur at the surface of the substrate (without participation of hot electrons), and these polymerization products can undergo further LDI and "electron capture dissociation". By comparing the Juglone testing results of ND and AgNI-on-ND (Figure 4), we can see that using ND as LDI-assisting material only generated a very small number of polymerized Juglone, about 30 times less than that of using AgNI-on-ND, indicating LSPR plays a major role in promoting polymerization. LSPR here has two effects, one is heating, the other is hot electron. These two effects contribute simultaneously to the formation of polymer, and it would be hard to tell which one contributes more. But this does not affect the fact that the ionization of all these molecules is the result of hot electron transfer, which is our main argument for this paper.

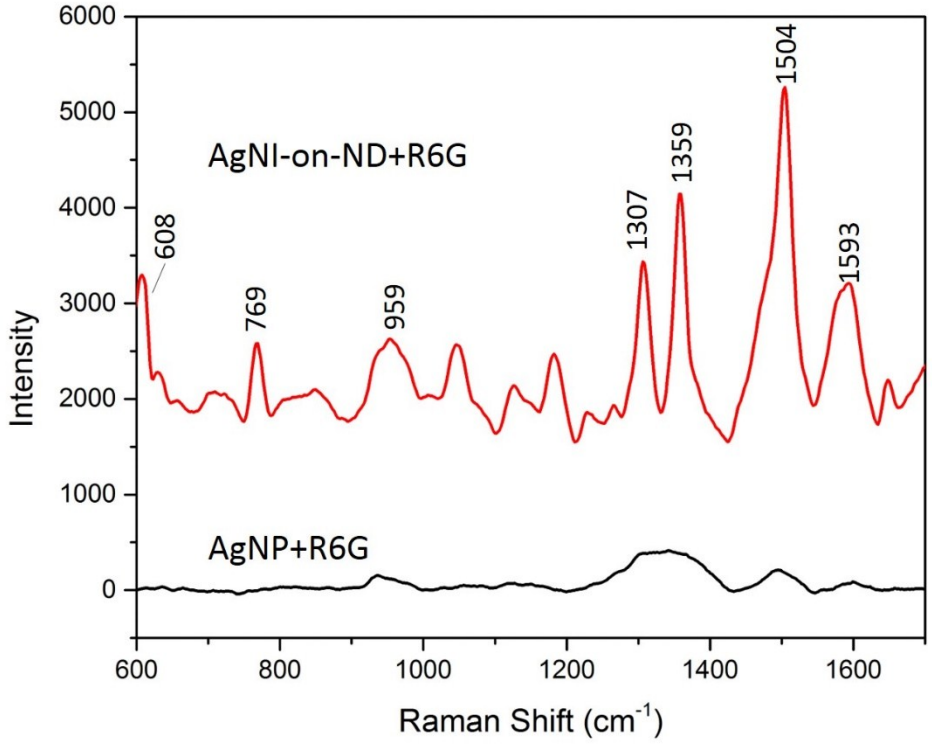

Figure S8. Raman spectra of 0.1 mM Rhodamine 6G (R6G) on AgNP and AgNI-on-ND respectively. Excitation wavelength was 785 nm.

The R6G signal obtained on AgNI-on-ND is about 6-10 times stronger than that obtained on AgNP, indicating AgNI-on-ND does have stronger LSPR effect than AgNP does. The signal enhancement factor is consistent with our LDI MS results.

Reference

1. Y.F. Li; J.N. Wang; L.P. Zhan; J.J. Xue; Z.X. Nie. Submitted.

2. Jin, Y.; Kang, X.; Song, Y.; Zhang, B.; Cheng, G.; Dong, S. *Anal. Chem.* 2001, **73** (13), 2843.

3. Frederix, F.; Friede, J-M.; Choi, K-H.; Laureyn, W.; Campitelli, A.; Mondelaers, D.; Maes, G.; Borghs, G. *Anal. Chem.* 2003, **75**, 6894.

4. R. A. Picca; C. D. Calvano; N. Cioffi; F. Palmisano, *Nanomaterials*. 2017, **7**.

5. Bohren, C. F.; Huffman, D. R. Wiley: New York, 1998.